JGR Biogeosciences

METHOD
10.1029/2022JG007200

Key Points:

- Fast in situ measurements of dissolved methane and its stable carbon isotope
- High-spatial resolution mapping of dissolved methane and its stable carbon isotope
- Improved production/oxidation process identification over discrete sampling

Supporting Information:

Supporting Information may be found in the online version of this article.

Correspondence to:

R. Grilli,
roberto.grilli@cnrs.fr

Citation:

Grilli, R., DelSontro, T., Garnier, J., Jacob, F., & Némery, J. (2023). A novel high-resolution in situ tool for studying carbon biogeochemical processes in aquatic systems: The Lake Aiguebelette case study. *Journal of Geophysical Research: Biogeosciences*, *128*, e2022JG007200. https://doi.org/10.1029/2022JG007200

Received 23 SEP 2022
Accepted 20 NOV 2023

Author Contributions:

Conceptualization: R. Grilli, F. Jacob, J. Némery
Data curation: R. Grilli, T. DelSontro, J. Garnier, F. Jacob, J. Némery
Formal analysis: R. Grilli
Funding acquisition: R. Grilli, F. Jacob, J. Némery
Investigation: R. Grilli, J. Némery
Methodology: R. Grilli, T. DelSontro, J. Garnier
Project Administration: J. Némery
Resources: R. Grilli, J. Garnier
Visualization: R. Grilli
Writing – original draft: R. Grilli, T. DelSontro, J. Garnier, J. Némery

A Novel High-Resolution In Situ Tool for Studying Carbon Biogeochemical Processes in Aquatic Systems: The Lake Aiguebelette Case Study

R. Grilli[1], T. DelSontro[2], J. Garnier[3], F. Jacob[4], and J. Némery[1]

[1]University of Grenoble Alpes, IRD, CNRS, INRAE, Grenoble INP, IGE, Grenoble, France, [2]Department of Earth and Environmental Sciences, University of Waterloo, Waterloo, ON, Canada, [3]Sorbonne Université CNRS EPHE, Milieux environnementaux, transferts et interactions dans les hydrosystèmes et les sols, METIS, Paris, France, [4]Centre d'Ingénierie Hydraulique, EDF, La Motte-Servolex, France

Abstract Lakes and reservoirs are a significant source of atmospheric methane (CH_4), with emissions comparable to the largest global CH_4 emitters. Understanding the processes leading to such significant emissions from aquatic systems is therefore of primary importance for producing accurate projections of emissions in a changing climate. In this work, we present the first deployment of a novel membrane inlet laser spectrometer (MILS) for fast simultaneous detection of dissolved CH_4, ethane (C_2H_6) and the stable carbon isotope of methane ($\delta^{13}CH_4$). During a 1-day field campaign, we performed 2D mapping of surface water of Lake Aiguebelette (France). Average dissolved CH_4 concentrations and $\delta^{13}CH_4$ were 391.9 ± 156.3 nmol L^{-1} and −67.3 ± 3.4‰ in the littoral area and 169.8 ± 26.6 nmol L^{-1} and −61.5 ± 3.6‰ in the pelagic area. The dissolved CH_4 concentration in the pelagic zone was 50 times larger than the concentration expected at equilibrium with the atmosphere, confirming an oversaturation of dissolved CH_4 in surface waters over shallow and deep areas. The results suggest the presence of CH_4 sources less enriched in ^{13}C in the littoral zone (presumably the littoral sediments). The CH_4 pool became more enriched in ^{13}C with distance from shore, suggesting that oxidation prevailed over epilimnetic CH_4 production and it was further confirmed by an isotopic mass balance technique with the high-resolution data. This new in situ fast response sensor allows one to obtain unique high-resolution and high-spatial coverage data sets within a limited amount of survey time. This tool will be useful in the future for studying processes governing CH_4 dynamics in aquatic systems.

Plain Language Summary High-resolution mapping of surface methane and its isotopic signature enables accurate characterization of aquatic systems and discrimination of biochemical processes at work. At Lake Aiguebelette, this new in situ tool allowed us to conclude that methane present at the surface comes mainly from shallow littoral areas, where sediments, which are a source of methane, are closer to the surface. During lateral transport of water masses from the littoral zone, the change in isotopic signature reveals that methane oxidation prevails over local in situ production. Comparison with previous studies validates the importance of high-resolution measurements (particularly to capture the high variability in the littoral zone) and showed that smaller lakes experience stronger methane isotopic signature changes for a given methane concentration variation. This can be explained by the fact that the smaller lake has a larger littoral-to-total surface area. This new tool will be useful in the nearby future to study the processes governing CH_4 dynamics in aquatic systems.

1. Introduction

Inland waters are a significant source of atmospheric methane (CH_4) (DelSontro, Beaulieu, & Downing, 2018; Rosentreter et al., 2021; Saunois et al., 2019), which is a greenhouse gas (GHG) 34–85 times stronger than carbon dioxide (on 100 to 20-year timescales including feedbacks; Myhre et al., 2013) and responsible for ∼23% of global radiative forcing since 1,750 (Etminan et al., 2016). Of the GHGs produced by inland waters (i.e., carbon dioxide, CH_4 and nitrous oxide), CH_4 is responsible for ∼75% of the climatic impact of aquatic GHG emissions (DelSontro, Beaulieu, & Downing, 2018) with aquatic CH_4 emissions comparable to the largest global CH_4 emitters - wetlands and agriculture (Saunois et al., 2019). Considering that aquatic systems contribute up to half of global CH_4 emissions (Rosentreter et al., 2021), and the fact that CH_4 is predominantly formed in anoxic environments such as lake sediments (Bastviken et al., 2004), the source and quantification of ubiquitous

Writing – review & editing: R. Grilli, T. DelSontro, J. Garnier, J. Némery

surface CH_4 observed in most aquatic systems are a question of global importance (e.g., Juutinen et al., 2009; Rasilo et al., 2015; Tranvik et al., 2009). As a result, monitoring of aquatic dissolved CH_4 concentrations and emissions has steadily become more commonplace, although the methods used, particularly for investigating concentrations, remain rather manual and laboratory oriented. Concentration alone may not always be sufficient for identifying the source of surface CH_4 and the isotopic signature and/or the measurement of other short-chain hydrocarbons can significantly help to unravel the origins of the dissolved CH_4 and identify processes through which the observed CH_4 pool was potentially metabolized (Claypool & Kvenvolden, 1983).

The headspace technique (McAullife, 1971) is the manual approach most used to sample for dissolved CH_4, with concentrations later measured on a gas chromatograph (e.g., Garnier et al., 2013; Rasilo et al., 2015). Because of the manual nature of these measurements, only a few or even just one sample is often taken in systems, particularly during multi-lake surveys (e.g., Rasilo et al., 2015). Recently, however, equilibrator systems have been used to extract dissolved gas from water (either in situ or on site) which is then directed either to a laser-based optical spectrometer (Gerardo-Nieto et al., 2019; Gonzalez-valencia et al., 2014; Grilli et al., 2020; Wankel et al., 2013; Yuan et al., 2020) or to a compact mass spectrometer (Bärenbold et al., 2020; Brennwald et al., 2016; Short et al., 2006) for highly resolved measurements. Note that this is a not extensive list of studies. Other commercial devices for in situ measurements of dissolved gases are also available. For example, the METS sensor from Franatech has the advantage of being compact, low cost, and easy to use, but it relies on an indirect technique that suffers from not being gas selective, which may lead to artifacts due to presence of other dissolved gas species or to the variability of other parameters related to the water mass (e.g., dissolved oxygen content, temperature, salinity, hydrostatic pressure). The HydroC Contros sensor from -4H-JENA relies on the measurement of partial pressure of the dissolved gases by a Tunable Diode Laser Absorption Spectroscopy (TDLAS) technique but suffers from a slow response time (t_{90} > 30 min for CH_4) due to the membrane equilibration approach, making fast dynamic measurements impossible.

Compact quadrupole mass spectrometers are now available and led to the development and commercialization of Membrane Inlet Mass Spectrometer (MIMS) devices. These instruments provide a fast response time and a large spectrum of gas species that can be simultaneously analyzed (Noble gases, N_2, O_2, CH_4, CO_2, H_2S, N_2O, etc.) (McMutrtry et al., 2005; Short et al., 2006; Tortell, 2005). However, the compactness of the device for in situ measurements limits the achievable mass resolution, leading to a problem of interference between fragments with similar mass, and making isotopic measurements still not conceivable.

With the advances on the development of optical spectroscopy sensors, and particular on cavity-based techniques, high precision concentration and also isotopic measurements are now possible using compact and transportable instruments (among others, commercial sensors including Picarro, Los Gatos Research, Thermo Scientific). When coupled with a dissolved gas extraction technique, these analyzers can provide in situ high-resolution isotopic gas measurements (Loken et al., 2019; Maher et al., 2015; Maier et al., 2022; Wankel et al., 2013; Webb et al., 2016).

It was long thought that the primary source of surface CH_4 was exclusively from anoxic sediments, either transported from littoral zones (Hofmann et al., 2010; Murase et al., 2003) or from pelagic sediments during non- or weakly stratified periods (MacIntyre & Melack, 1995). In stratified systems, CH_4 produced in anoxic sediments diffuses into and accumulates in bottom waters but is trapped beneath a zone of minimal diffusion (Vachon et al., 2019) and oxidation (Bastviken et al., 2008), which is the primary sink for dissolved CH_4. This begs the question whether littoral sediments can adequately supply most of the surface CH_4 observed particularly in large and stratified lakes. Recent evidence suggests that CH_4 can also be produced in surface oxic waters (Bižić et al., 2020; Grossart et al., 2011) at rates sufficient enough to maintain surface CH_4 pools in a variety of systems and contribute significantly to atmospheric emissions (Günthel et al., 2019). Mass balance exercises in some systems have supported the notion that oxic methane production (OMP) can supply the majority of surface CH_4 during the stratified period (Donis et al., 2017). However, it is likely that both transport from littoral sediments and OMP maintain the surface CH_4 supply in at least most smaller lakes (DelSontro, del Giorgio, & Prairie, 2018). Measurements of $\delta^{13}C$ of CH_4 have provided further evidence that surface CH_4 is not only sourced from bottom waters (e.g., Donis et al., 2017; Ordóñez et al., 2023) and that oxidation and an addition from another CH_4 pool (i.e., OMP) modulates the observed CH_4 pool in surface waters (DelSontro, del Giorgio, & Prairie, 2018). High resolution $\delta^{13}C$ measurements have the potential to offer significantly more information regarding CH_4 sources and processing in freshwaters than concentrations alone, but fast responding and high-resolution instruments for measuring $\delta^{13}C$ are lacking.

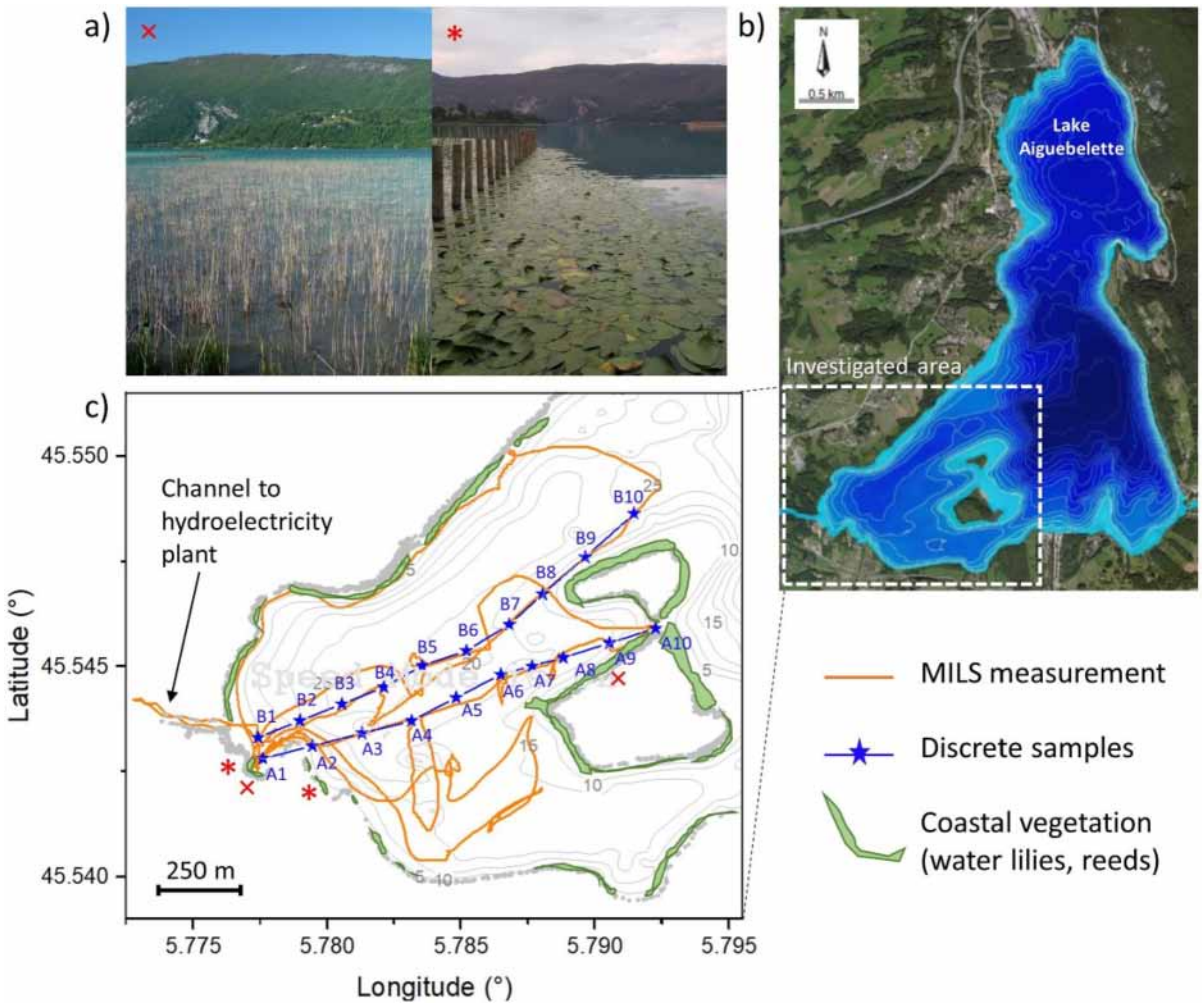

Figure 1. (a) Two pictures of the vegetation: left panel: reeds, taken near sampling point A8—A9; right panel: water lilies taken near sampling location A1; (b) A large satellite view of Lake Aiguebelette with the bathymetry highlighted by 5-m isobar lines and shades of blue (source EDF); (c) A zoom on the investigated area with the trajectories of the in situ MILS sensor (orange line), the location of the discrete samples along two legs (blue stars), and the coastal vegetation (green).

In this work, we present a first deployment of a novel membrane inlet laser spectrometer (MILS) instrument that is an upgraded version of the SubOcean probe (Grilli et al., 2018, 2020; Triest et al., 2017). A newly developed mid-infrared spectrometer for simultaneous detection of CH_4, C_2H_6 and $\delta^{13}CH_4$ (Lechevallier et al., 2019) was implemented on the in situ instrument. Laboratory calibrations of the sensor are reported in the method section, followed by the results and discussions about the dissolved CH_4 data from the field campaign at Lake Aiguebelette (south east of France). Besides proving the interest of our new deployed methodology on the Lake Aiguebelette, our field investigations aimed at providing reference data on this natural peri-alpine lake in terms of CH_4 level and transformations based on associated $\delta^{13}C$ determinations.

2. Materials and Methods

2.1. Study Area and Field Setup

The natural peri-alpine Lake Aiguebelette is located in the northern French Alps (45.5578°N, 5.8014°E) at an altitude of 374 masl (Figure 1). The region has a sub-continental climate with mean annual rainfall of 1,311 mm, and mean monthly air temperature fluctuates between 1.6 and 24°C (OLA, 2022). The lake has a total volume of 166×10^6 m^3 with a surface area of 5.45 km^2 for a maximum and mean depth of 70 and 30.7 m, respectively (Rimet et al., 2020). The upstream watershed surface is 59 km^2 and the water of the lake flows through the channel of Thiers to a hydroelectric plant. The lake outflow is regulated by the French Electricity Company (EDF), leading to regular fluctuations of lake level up to 0.5 m.

The lake is a warm monomictic lake that stratifies from April to November and has a mean water residence time of 3.1 years. Epilimnion depth reaches 10 m during the summer period when the hypolimnion has oxygen concentrations <1 mgO_2 L^{-1} (Rimet et al., 2020). Like other peri-alpine lakes such as Geneva, Bourget and Annecy, Lake Aiguebelette experienced eutrophication during the 1960s and 1970s due to urbanization and touristic development. The site is now a natural area of ecological, faunistic and floristic interest listed as Natura 2000 since 2006 (NINH, 2016). A large part of the coastline (<6 m water depth) is a protected natural reserve and has experienced the regeneration of a large band of macrophytes (11.8 ha) dominated mostly by reeds *(Phragmites australis*), with water lilies (*Nuphar lutea* and *Nymphaea alba*) present preferentially in the southern coast of the lake (2.4 ha). The southern coast is also more urbanized than the northern coast of the studied area (CCLA, 2017).

The measurements were carried out on 15 May 2019 at the end of a 15-day period of activity at the hydroelectric station that lowered the water level by ∼0.4 m. The continuous high-resolution MILS measurements were performed on a small electric boat equipped with GPS positioning (Garmin 18×, with an accuracy of 15 m, 1σ). The boat route explored the shallow areas near the shore in the southwest of the lake to the islands in the center of the lake, then into the channel of Thiers at the lake outlet (Figure 1). The MILS system provided real-time data on the boat, allowing us to adjust the path during the campaign. A second electric boat not equipped with GPS followed the course of the first boat on legs A and B (Figure 1) in order to collect discrete water samples at 20 locations to help validate the MILS measurements. For the discrete samples, 100-ml of water was collected in a glass flask at 0–30 cm below the surface without air bubbles. To stop biological activity, three drops (50–80 µl) of a solution of $HgCl_2$ (i.e., 2.5%–4% in final concentration) was added and the glass flask was sealed with a rubber septum excluding any headspace gas in the field. Measurements of physiochemical parameters were realized using a multi-parameter probe (WTW 3420®), such as, temperature, pH, conductivity, dissolved oxygen concentration and percentage of oxygen saturation.

2.2. The MILS In Situ Sensor

The MILS used here is an upgraded version of the existing SubOcean sensor that was fully described in Grilli et al. (2018). It relies on a patent-based extraction system for fast response measurements (Triest et al., 2017). The optical spectrometer, based on the optical feedback—cavity enhanced absorption spectroscopy (OFCEAS) technique (Morville et al., 2014) was working in the mid-infrared region at 3.3 µm for simultaneous detection of CH_4, C_2H_6 and $\delta^{13}CH_4$ (Lechevallier et al., 2019). The entire sensor was installed on the boat, and only the extraction unit was immersed in the water at ∼50 cm depth (see Figure S1 in Supporting Information S1). The latter is composed by two 10 µm thick polydimethylsiloxane (PDMS) membranes (56 mm diameter) mounted face-to-face in a stainless-steel housing. The membrane block (MB) was connected to a submersible water pump (Sea-Bird Electronics, SBE 5T) that enables flushing of the membranes with a water flow of 0.8 L min^{-1}. The extraction unit was attached to the boat and connected to the probe with two 1/8," 1.2-m long flexible perfluoroalkoxy (PFA) gas pipes. A second pipe was used to inject a known flow of carrier gas (Zero Air, ALPHAGAZ 2, Air Liquide) on the dry side of the membranes. This has various purposes: (a) increase the flow of gas to analyze, (b) flush the membrane in order to maintain the maximum partial pressure difference of the target gases across the membranes (both points increase the response time of the measurement); and (c) apply a dilution to the extracted gas to increase the dynamic range of the measurement and optimize in real time the concentration of CH_4 for the isotopic measurement. The carrier gas was stored in a 1L stainless-steel tank and a pressure reducer (Pred) and mass flow controller (MFC_{CG}, IQF+, Bronkhorst) were used for generating a controlled and constant flow of dry carrier gas. The total flow coming from the extraction system, composed of the dry dissolved gas, water vapor and carrier gas, was measured by a second mass flow controller (MFC_{TF}, IQF + Bronkhorst) and then sent to the optical spectrometer. Prior to the MFC_{TF} a 3-port, 2-position switch valve (Burkert 6014, SV) was used for injecting from time to time a standard gas for calibrating the isotopic measurement. During the measurements, the setpoint of the MFC_{TF} was set to 10 sccm (standard cubic centimeter per minute) allowing to use it as a flow meter and to 1.3 sccm during the standard gas measurement. Data were acquired at 4 Hz, and averaged to 2 and 20 s for concentrations and isotopic ratio measurement, respectively.

2.3. Laboratory Analysis and Validation of the MILS Instrument

From the 20 discrete samples collected, concentrations of CH_4 were determined by gas chromatography with flame ionization detection (Clarus 580, PerkinElmer) after creating a 30-mL headspace with N_2, as described in

(Abril & Iversen, 2002; Koné et al., 2010). Certified CH_4:N_2 mixtures at 10 and 500 ppm of CH_4 were used as standards (Air Liquide, France). Repeatability was around ±5% (2σ). Dissolved CH_4 concentration was calculated with the solubility coefficient provided by Sander (2015).

The setup used to calibrate the MILS instrument in the laboratory is fully described in Grilli et al. (2018). Similar to the field application, the extraction unit is installed in a temperature stabilized chamber and immersed in ∼10 L of water. A gas mixture at known concentration of CH_4 in air is bubbled in the water by a diffuser, and the dissolved gas concentrations were monitored continuously with the optical spectrometer. For CH_4 concentration measurements, the membrane efficiency was calculated at different water temperatures (4–22°C) and salinities (0–31 psu) (reported in Grilli et al., 2018) and the concentrations of dissolved CH_4 were calculated from the solubility coefficients provided by Sander (2015). The measurements of C_2H_6 are reported in Figure S2 in Supporting Information S1. Concentrations of dissolved C_2H_6 are in ppm and were calculated using the membrane permeation coefficient published by Robb (1968) and following the same procedure as for CH_4. Because of the low variability of dissolved C_2H_6 observed during the campaign, discussions are limited to CH_4 and $\delta^{13}CH_4$ measurements. Salinity and dissolved oxygen content play a role in retrieving dissolved gas concentrations and they must be known; however, they do not affect the isotopic measurement (see the SI for more information). The effect of turbidity of the water as well as the fouling of the membrane have not been studied so far and would require further investigations.

Isotopic accuracy of the in situ instrument was assessed from three lab-derived accuracies: (a) the accuracy and long-term stability of the optical spectrometer, (b) the accuracy related to the correction due to the concentration dependency of the isotopic measurement; and (c) the correction due to the water temperature-based membrane fractionation. For the calibration of the isotopic measurement, three reference standards of −38.3, −54.5, and −66.5‰ VPDB (Isometric Instrument) were used. As observed previously (Lechevallier et al., 2019), the isotopic signature shows a dependency on CH_4 concentrations with a deviation from the true value at lower concentrations. This deviation has to be removed while retrieving the isotopic value by using the exponential function from the calibration curves reported in Figure 2a. Here $\delta^{13}CH_4$ is calculated from $R^{13}C$ using Equation 1, and the $R^{13}C$ are the measured and reference ratios between the $^{13}CH_4$ and $^{12}CH_4$ absorption lines.

$$\delta^{13}CH_{4\,\mathrm{meas/VPDB}} = \frac{R^{13}C_{\mathrm{meas}}}{R^{13}C_{\mathrm{ref}}} \times \left(1 + \delta^{13}CH_{4\,\mathrm{ref/VPDB}}\right) - 1 \quad (1)$$

where $R^{13}C_{meas}$ and $R^{13}C_{ref}$ correspond to the relative $^{13}C/^{12}C$ abundance ratios measured by the instrument for the measured and reference gas, respectively, and $\delta^{13}CH_{4\,ref/VPDB}$ is the isotopic value for the reference mixture certified against a standard material (in this case *Belemnitella americana* fossil carbonate, Vienna Pee Dee Belemnite scale). This means, for instance, that one can compute the $\delta^{13}CH_4$ for the standard at −66.5‰ by using the measured $R^{13}C$ and the certified $\delta^{13}CH_4$ of the −38.3‰ standard that will act as a reference. From the residuals between the measurement data points and the exponential fits in Figure 2a we estimated a maximum contribution by this calibration of ±1.4‰ (2σ) to the final accuracy of the measurements.

In order to prove the long-term stability of the system for retrieving the isotopic signature of CH_4, we performed the measurements of the three isotopic standard mixtures at ∼100 ppm of CH_4 during different days. Between each series of measurements, the instrument was switched off. The results are reported in Figure 2b. $\delta^{13}CH_4$ values were obtained by applying Equation 1 to the $R^{13}C$ data. The corresponding variability in the $\delta^{13}CH_4$ ranged between ±4 and ±6.6 ‰ (2σ), which represents the accuracy of the optical spectrometer on the $\delta^{13}CH_4$ unreferenced to a measured standard mixture. This accuracy can be reduced to ±0.4‰ (2σ) by averaging the data for ∼10 min (Figure 3 in Lechevallier et al., 2019), but also by injecting a reference gas standard for a further ∼10 min in order to prevent the accuracy of the measurement to be degraded by instrumental drifts. This, however, is at the price of degraded spatial resolution of the measurements. The same figure in Lechevallier et al. (2019) shows as well that when data were acquired by locking the cavity modes with respect to the position of the absorption lines (which was the case for the field campaign at Lake Aiguebelette), the spectrometer exhibits a much longer stability. Despite long-term drifts that start to arise after ∼17 min, the precision of the measurement stays below ±2‰ (2σ) for 12hr and ±1.6‰ (2σ) during the 9h of continuous measurement (corresponding to the time of the survey) (Lechevallier et al., 2019).

For an accurate isotopic measurement, water conditions also have to be considered because a change in the water temperature will affect the isotopic fractionation at the membrane. This is related to the fact that after adsorption

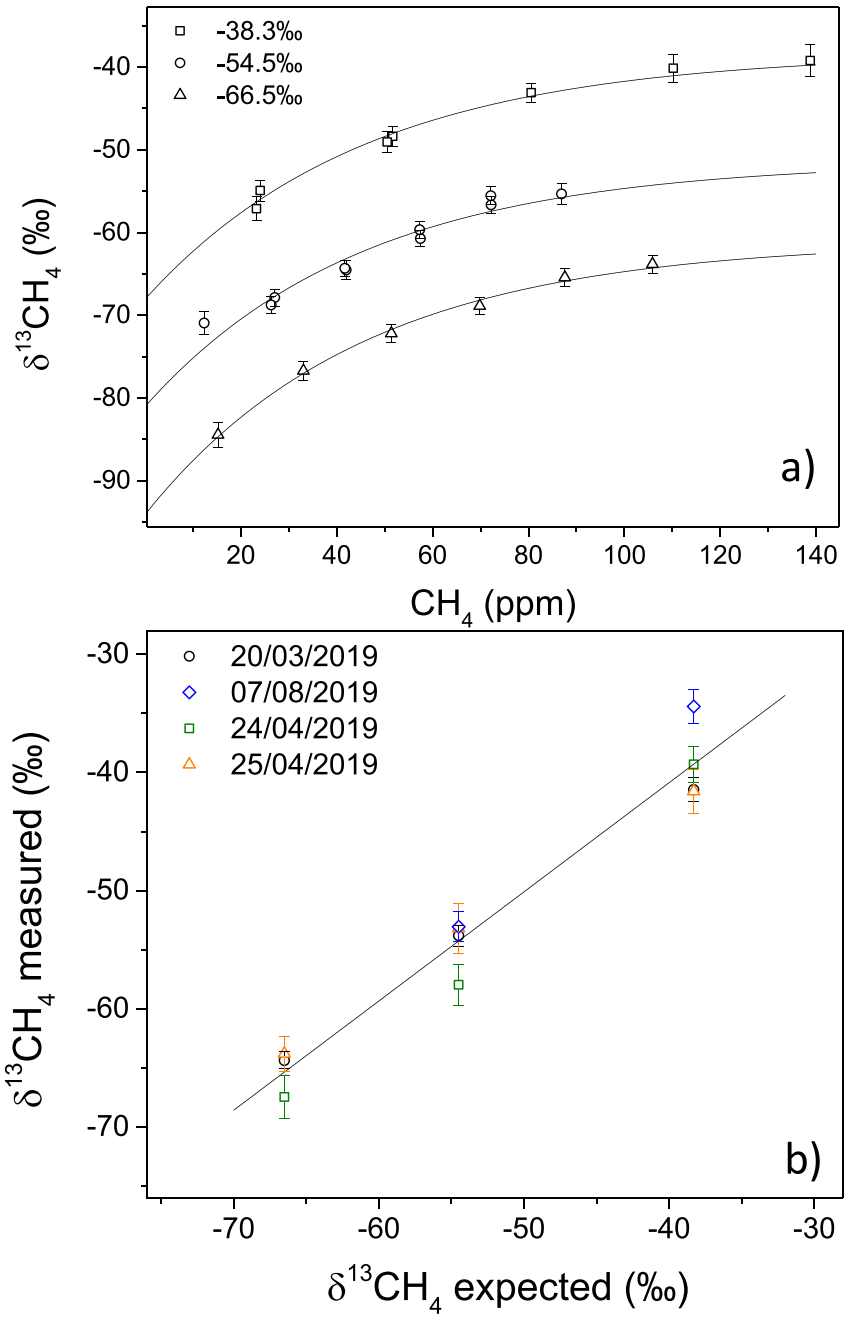

Figure 2. (a) Calibration curves of the optical spectrometer for three isotopic standard mixtures showing the dependency of the abundance isotopic ratio with the concentration of CH_4. This dependency is due to an instrumental (spectral fit related) artifact that has to be considered while retrieving the $\delta^{13}CH_4$ values. (b) A long-term stability test of the optical spectrometer. Measurement of the three standard mixtures was performed at different days. The spectrometer was switched off between each series of measurements. $\delta^{13}CH_4$ values were calculated using Equation 1, by taking the average $R^{13}C$ of the −54.5‰ as a reference standard mixture values. It should be noted that, because an average $R^{13}C$ was used as reference for the whole sets of measurements, the scattering of the datapoints represents the worst precision one can expect. Error bars represent the standard error (2σ) of the measurement for 20 s acquisition.

and permeation through the membrane, the gas will be desorbed, which is equivalent to an evaporative process causing a mass dependent fractionation. This effect was estimated in the laboratory using the same calibration setup explained above. In the water where the MB was submerged, a gas mixture with a known concentration and isotopic signature of dissolved CH_4 in dry air was continuously bubbling while tuning the water temperature from

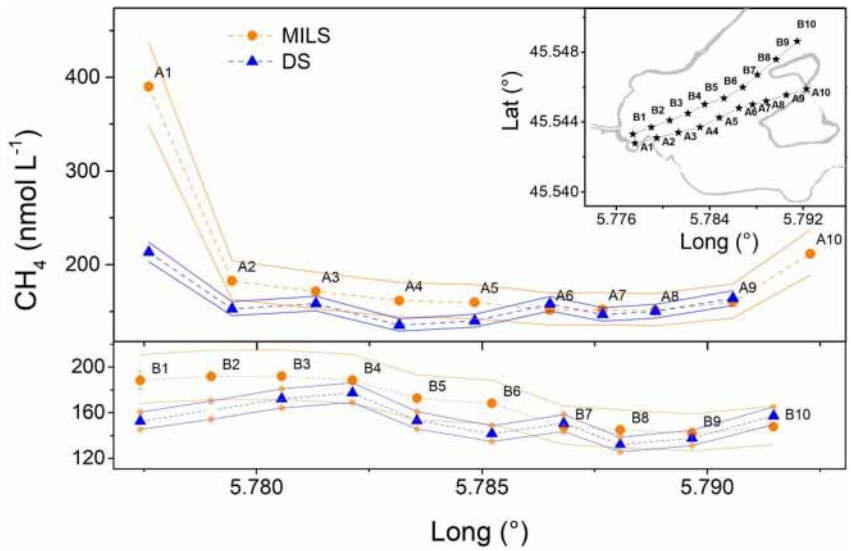

Figure 3. Comparison of dissolved CH_4 measurements performed by the standard methods (discrete water sampling, DS, followed by laboratory headspace analysis, blue triangles) and in situ measurements performed by the MILS instrument (orange dots) along A and B legs. Error bars of ±5 and ± 12% (2σ), respectively, are reported by solid lines and discussed in Section 2. In the insert, the map shows the sampling and measurement locations (black stars) as well as the margins of the basin (in gray).

23 to 8°C and continuously monitoring the $R^{13}C$. The results are reported in Figure S3 in Supporting Information S1 and show an effect of the water temperature on the isotopic measurement of 0.6‰ per °C on the $R^{13}C$, which corresponds to 0.9 ‰ per °C on the $\delta^{13}CH_4$. The calibration was less critical for this particular campaign since the instrument only measured surface water with a stable temperature of 14.5 ± 0.2°C during the entire campaign, which corresponds to an added uncertainty of ±0.4‰ (2σ) to the final accuracy estimation of the $\delta^{13}CH_4$ measurement.

Based on the dependency of the $\delta^{13}CH_4$ on the CH_4 concentration and water temperature as well as on the repeatability of the $\delta^{13}CH_4$ measurements, the final accuracy of the in situ $\delta^{13}CH_4$ measurements estimated from laboratory characterization is ±2.2‰ (2σ, calculated as the root of the sum of squares of the three lab-derived accuracies detailed above: ±1.6‰ for the uncertainty coming from the spectrometer, ±1.4 ‰ due to the concentration dependency, and ±0.4 ‰ due to the water temperature-based membrane fractionation), while accuracy of the measurement of dissolved CH_4 concentration was previously estimated as ±12% (2σ), largely limited by the accuracy on the measurement of the carrier gas and total gas flows (Grilli et al., 2018). It should be noted that those accuracies were estimated by laboratory calibrations and do not account for possible degradations due to field operation. The accuracy of the instrument in the field is addressed in the following section.

2.4. Performance of the MILS Sensor in the Field: Reproducibility and Comparison With Discrete Measurements

During the field campaign, water sampling was conducted at different locations along two legs (Figure 1c) and analyzed in the laboratory by the headspace technique in order to compare the results with the in situ dissolved gas measurements performed by the MILS sensor (Figure 3). The two data sets are generally in good agreement, except for at A1 where the MILS observed a higher dissolved CH_4 concentration than the discrete water sample analysis (390.1 ± 46.8 and 213.5 ± 10.7 nmol L^{-1}, respectively). This may be explained by different reasons. First, the discrete water sampling was performed with a second boat not equipped with a GPS unit that was following the course of the first boat; therefore, the two concentrations may not have been observed at the exact same location. Figure 4a emphasizes this point as one can see the strong heterogeneity in surface water CH_4 content within 20 m distance. Thus, even small offsets in location would be critical for method comparison in nearshore zones due to the strong variability of surface dissolved CH_4 concentrations. Position accuracy becomes less critical further away from the shore as concentrations decrease (Figure 4b). A second possible reason for the

discrepancy at A1 (Figure 3) comes from the fact that the extraction unit for the MILS sensor was at 50 cm depth, while discrete water sampling was performed between 0 and 30 cm depth. This 20–50 cm difference in sampling depth is likely to cause discrepancies between methods when sampling at shallower nearshore depths where, as already stated, large concentration gradients can be present. Finally, the discrepancy could also be related to a combination of the two hypotheses. Figure 3 highlights the limitation of a discrete (low-resolution) measurement approach. The high variability found in the littoral with the highly resolved data presented in this work was not captured by discrete measurements, and the concentration gradient while going from the littoral to the pelagic zone using discrete measurements would only rely on a single measurement point (location A1, Figure 3). Thus, high CH_4 concentrations and trends would be missed and lead to different interpretations if minimal sampling (either spatially with in situ sensors or via discrete measurements only) were used. The choice of the sampling location in the littoral zone is critical, and high-resolution mapping is an effective solution for a more representative data set. The same could be said about the isotopic measurements.

Note that the maximum depths below the two surface transects are similar for both transect legs (see Figure S6 in Supporting Information S1) and CH_4 concentrations in those transects also follow a similar pattern.

Reference standard gas measurements with the embedded gas standard mixture (see the description of the MILS sensor in Section 2.2) were conducted with the MILS instrument during the field campaign at different times of the day and reported in Figure S4 in Supporting Information S1. The standard deviation of these reference measurements was ±4‰ (2σ), which agrees relatively well with the ±2.2‰ (2σ) accuracy mentioned above and resulting from the laboratory calibration experiments and propagation errors. This confirmed that the optical spectrometer was sufficiently stable over the 9h of survey.

At 4:37 p.m. local time, we traveled ∼320 m into the narrow channel on the South-West side of the basin that leads to the hydroelectric plant, and then returned along almost the same exact track over a 15-min period (Figure S5 in Supporting Information S1). The similarity in concentration and isotopic results reported in Figure S5 in Supporting Information S1 highlights the good reproducibility of the sensor in real conditions.

At the entrance of the channel (right-hand side of the lower plots in Figure S5 in Supporting Information S1), the isotopic signature shows a discrepancy up to 3‰. This discrepancy, however, is not far from the accuracy of the instrument for the measurement of the $\delta^{13}CH_4$, and could also be related to a change in water mass at the entrance of the channel between the beginning and the end of the profile. It should be noted that during the measurements the hydroelectric plant was discharging water at about 1 $m^3\ s^{-1}$. Despite that minor discrepancy in the $\delta^{13}CH_4$, good reproducibility in both dissolved CH_4 and $\delta^{13}CH_4$ measurements was observed from the record in the channel.

In Figure 2, error bars represent the 2σ standard error (i.e., the standard deviation of a single measurement divided by the square-root of the number of average), which corresponds to the precision of the measurement, since over 20 s the noise is dominated by the white noise component. At 20 s averaging time, the precision of the instrument matches the accuracy during long-term measurements (±2.2‰ (2σ) for 9h survey as estimated from laboratory calibrations). Averaging for longer time will further improve the precision on a single measurement, but not the final accuracy unless regular measurements of a reference standard gas mixture are performed at the price of a poorer temporal resolution of the data.

In order to estimate the accuracy of the instrument in the field, a statistical analysis on the 20 s averaged $\delta^{13}CH_4$ in situ data from the pelagic zone only (distance from shore >75 m, Figure 5) was performed and a standard deviation of ±2.6‰ (2σ) was calculated, which agrees well with the accuracy of the instrument estimated in the laboratory.

It should be noted that this accuracy on the $\delta^{13}CH_4$ measurement requires a daily calibration with a standard gas mixture, otherwise a degradation from ±2.6 to ±6.6‰ (2σ) will occur, as reported in Figure 2b.

3. Results and Discussion

3.1. Spatial Distribution of CH_4 and $\delta^{13}CH_4$ in Lake Aiguebelette

The 2D maps in Figure 4 report the spatial variability of the dissolved CH_4 and its isotopic signature. The thickness of the colored line was chosen in order to have a better graphical visualization, while trying to be realistic

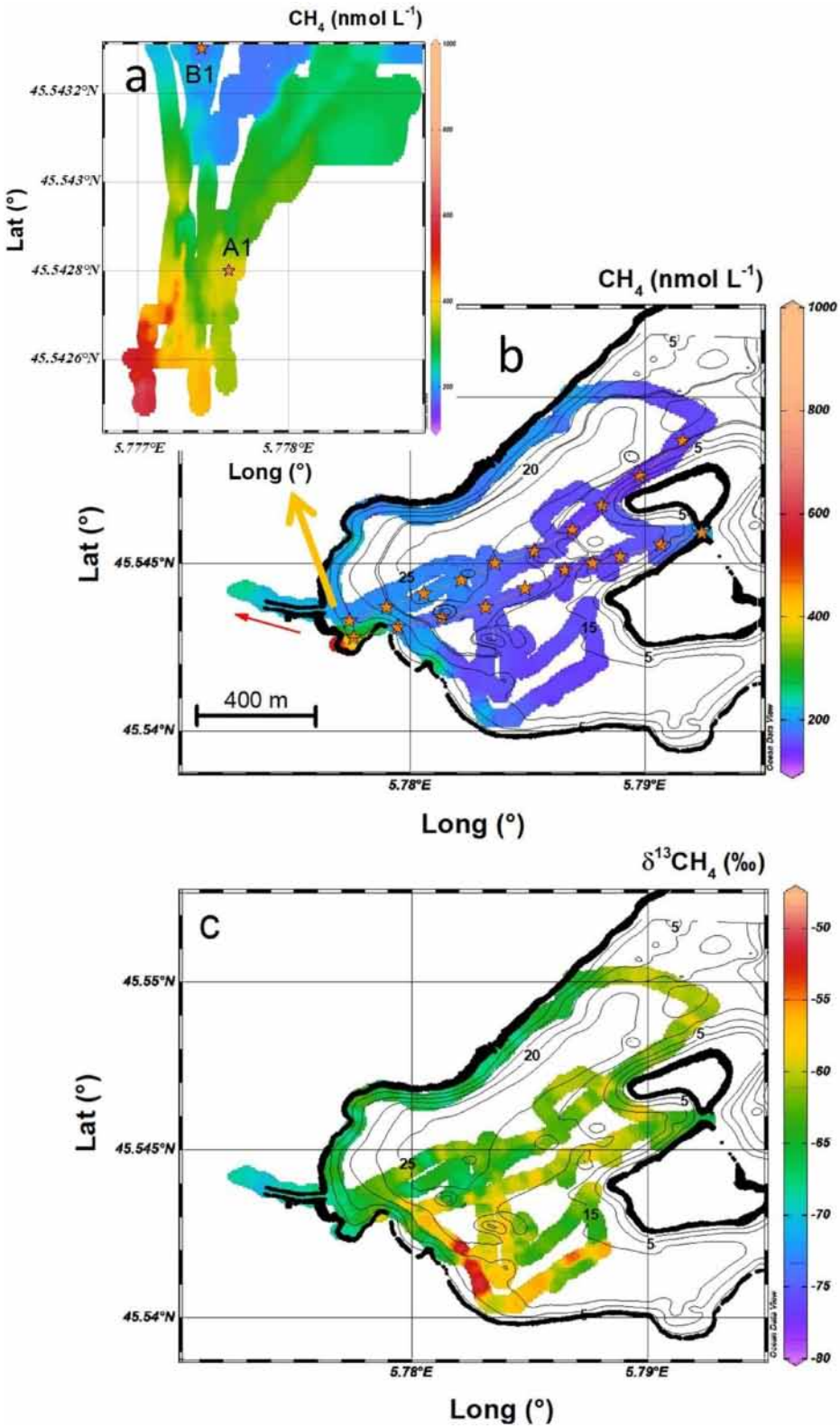

Figure 4. 2D maps of the dissolved CH_4 concentrations (a) and (b) and $\delta^{13}CH_4$ (c). The red arrow indicates the water flow in the exit channel of the lake and the orange stars the location of the discrete water samplings. Orange arrow indicates that (a) is a zoom of the area near sampling station A1 with high dissolved CH_4 concentrations and the highest concentration gradients. Black dots in (b) and (c) are the <1m depth contour line, which we defined as the shoreline.

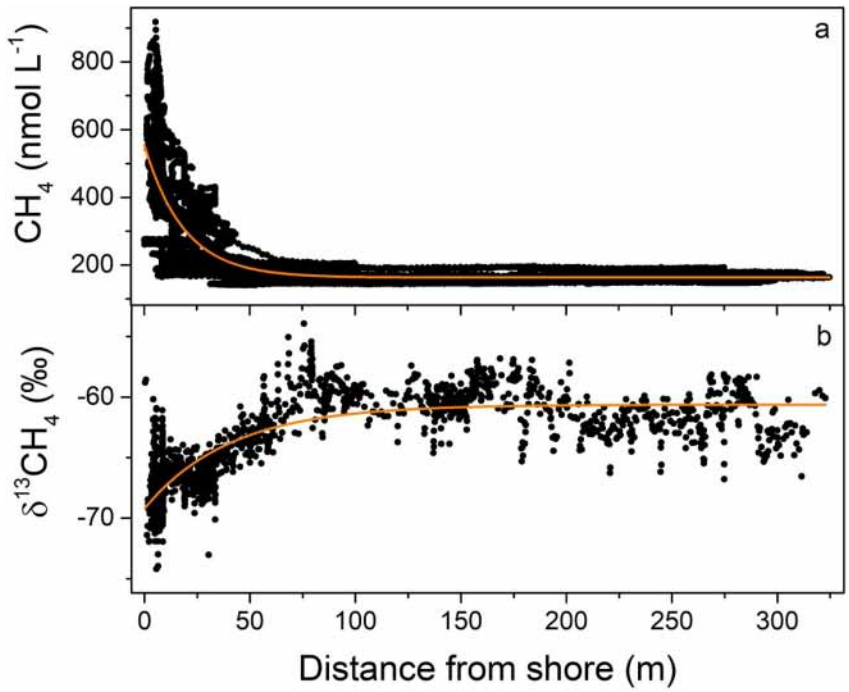

Figure 5. Distance from shore. Black dots are 2 s data for CH_4 (a) and 20 s data for $\delta^{13}CH_4$ (b), orange lines are exponential fits with exponential constant of 18.8 m^{-1} and −40.7 m^{-1} for the CH_4 and $\delta^{13}CH_4$ trends, respectively. The data from the channel were omitted for this figure.

with the possible uncertainty in the GPS position (~15 m, 1σ). Dissolved C_2H_6 was also measured simultaneously, but the 2D map is not reported since the signal was very stable over the entire campaign with a mean value of 2.0 ± 0.1 nmol L^{-1}. Dissolved C_2H_6 does not correlate with either the concentration of dissolved CH_4 or the $\delta^{13}CH_4$. The shore of the lake was defined by where water depth was <1m (black dots in Figure 4).

All observed dissolved CH_4 concentrations were above saturation in our study area. The dissolved gas concentration in the pelagic zone, where concentrations were the lowest observed, is 50 times larger than the concentration of dissolved gases expected at equilibrium with the atmosphere (3.4 nmol L^{-1} at survey temperature of 14.5°C).

The highest concentrations of dissolved CH_4 (400–920 nmol L^{-1}) were observed along the shore southeast of the channel in a small bay (red area on Figure 4a) and corresponded with slightly more negative $\delta^{13}CH_4$ values (−68.6 ± 3.3‰) with respect to the average value in the pelagic zone (−60.7 ± 1.4 ‰). In this area at shallow depths (<3 m) spontaneous ebullition was observed, which explains both high CH_4 concentrations and a more negative isotopic signature. Further southeast of that location and ~80 m offshore was an area with the most enriched $\delta^{13}CH_4$ values (−51.3 ± 1.3‰; red patch in the Figure 4c) and relatively low dissolved CH_4 concentrations (155.0 ± 3.5 nmol L^{-1}), although it was situated between two locations with elevated dissolved CH_4 concentrations (200–300 nmol L^{-1}). The ^{13}C-enrichment in this area may be related to a stronger biological activity, which may be due to the urbanization of this coastal area or to the presence of a large and dense patch of macrophytes (water lilies, see picture in Figure 1a). Water lilies are also present near the sampling location A1, but in this area an isotopic composition closer to the one expected in the sediments was found, most probably due to presence of gas ebullition. On the north shore of the lake, concentrations were consistently higher (192 ± 7 nmol L^{-1}), and $\delta^{13}CH_4$ more negative (−65.9 ± 1.8‰) than the average concentration and isotopic composition near the islands and in the middle of the lake (147.2 ± 3.4 nmol L^{-1}; 61.4 ± 1.8‰). On average, the CH_4 concentrations in the pelagic zone (>75m from shore) were 2.7 times lower (37%) than in the littoral zones (<10m from shore) of the study area (160.8 ± 14.2 nmol L^{-1} vs. 435.0 ± 174.5 nmol L^{-1}, respectively, Table 1), while the lightest $\delta^{13}CH_4$ values were in the northern part of the study area along the shore and the heaviest in the southern part just offshore.

Littoral zones of most lakes tend to be hot spots of CH_4 production, accumulation, and emission for several reasons. First is that shallow waters allow for warming of surface sediments and consequent production (Yvon-Durocher

Table 1
Average (Minimum, Maximum) Concentrations, Isotopic Composition and Water Depths for the Entire Survey Area, the Pelagic and the Littoral Zones

		Avg CH_4 (nmol L^{-1})	Avg $\delta^{13}CH_4$ (‰)	Water depth (m)
	Entire Survey Area	256.4 ± 147.3	−63.7 ± 4.5	11.6 ± 8.4
		(140.6; 922.4)	(−77.6; −49.6)	(1; 26.5)
Littoral Zone	<6 m water depth	391.9 ± 156.3	−67.3 ± 3.4	2.5 ± 1.6
		(158.8; 922.4)	(−77.6; −57.0)	(1; 6)
	<10 m from shore	435.0 ± 174.5	−67.6 ± 3.7	1.3 ± 0.5
		(165.0; 922.4)	(−77.6; −57.5)	(1; 7.6)
Pelagic Zone	>6 m water depth	169.8 ± 26.6	−61.5 ± 3.6	17.3 ± 5.4
		(140.6; 339.3)	(−73.2; −49.6)	(6; 26.5)
	>75 m from shore	160.8 ± 14.2	−60.7 ± 3.3	19.8 ± 3.7
		(142.6; 208.5)	(−69.0; −49.6)	(4.8; 26.5)

Note. Error bars on means correspond to ±1σ values.

et al., 2014). While degradation rates are likely slow during cold winter temperatures, decomposition rates start to increase as spring temperatures begin to warm the shallow littoral sediments first. Thus, our May campaign led to rather high CH_4 concentrations, possibly an order of magnitude higher than what would have been observed in winter (cf. Zhang et al., 2021). Secondly, littoral zones tend to be CH_4 hot spots because the shallow sloping sediments of a littoral zone, such as that of our study area, can be a receptacle for organic carbon from algal and macrophyte biomass throughout the growing and dying seasons. This increase in organic substrate, combined with warm temperatures, leads to higher rates of methanogenesis than the pelagic. The littoral zone of Lake Aiguebelette and the islands have indeed a large band (from 5 to 25 m wide) of rooted emergent aquatic macrophytes such as water lilies and reeds (density between 100 and 400 rods) (CCLA, 2017).

The productivity of littoral macrophytes has major implications for CH_4 release through the accumulation of detrital organic matter in sediment (Desrosiers et al., 2022; Juutinen et al., 2003). The increase of organic content in sediment of the macrophyte regions during and following the growing period can lead to intense mineralization and depletion of oxygen in sediment (Gaillard et al., 1987; Milberg et al., 2017; Phillips et al., 2013), conditions favorable for methanogenesis. Conversely, in the deeper part of the lake that has a lower sediment surface-to-water volume ratio than the littoral, less organic carbon would reach the bottom, of which some of it would already be partially aerobically decomposed (Steinsberger et al., 2020). As the bottom water of Lake Aiguebelette is still somewhat oxic (~3 mg/L), significant aerobic degradation would occur during particle settling and even in the slightly oxic surface sediments. Although, in general, decomposition will remain slow in the consistently cold bottom waters of this 70 m deep lake (Gudasz et al., 2010), and much of the CH_4 that is produced and then released will likely be oxidized (Bastviken et al., 2002). Ultimately, this type of functioning would support relatively low CH_4 concentrations for most of Lake Aiguebelette surface water, except for the shallow littoral zones as highlighted by our measurements. Based on all the preceding reasoning, we assume that any differences in the surface CH_4 concentrations would mostly be due to advection from the higher concentrated littoral zones as well as surface conditions impacting mixing and gas evasion.

3.2. Isotopic Signature for Identification of Biogeochemical Processing

The light isotopic signature of the CH_4 along the northern shore of the study area reflects fresh CH_4 production in the littoral zone, whereas the slightly heavier CH_4 pool toward the islands reflects oxidized CH_4, both of which are consistent with what has been observed elsewhere (e.g., DelSontro, del Giorgio, & Prairie, 2018). We therefore investigated the relationship between CH_4 concentration and $\delta^{13}CH_4$ with the distance from shore (DelSontro, del Giorgio, & Prairie, 2018). Two trends are shown in Figure 5: (a) both CH_4 and $\delta^{13}CH_4$ are relatively flat and constant at distances >75 m from the shore with average values of 160.8 ± 14.2 nmol L^{-1} and −60.7 ± 3.3‰, respectively; (b) CH_4 then rapidly increases near the shore, showing a larger scattering at a distance <10 m, with an average of 435.0 ± 174.5 nmol L^{-1}, highlighting that a large variability can be found nearby the shore

depending on the type of sediments and vegetation as well as variability in the water depths (this is also visible in the 2D map of Figure 4a). The $\delta^{13}CH_4$ starts to decrease at distance <75m, and it also shows a larger scattering of the data at a distance <10 m, with a mean value of $-67.6 \pm 3.7‰$.

The decreasing concentration with distance from shore (Figure 5-a) indicates that CH_4 sources are closer and/or more intense in the littoral zone. The presence of a CH_4 pool nearshore that is less enriched in ^{13}C (Figure 5b) further supports the concentration trend, that is, indicating that littoral waters are closer to CH_4 sources, which are presumably the littoral sediments. Seeing as this nearshore water can be advected offshore, the fact that the CH_4 pool becomes more enriched in ^{13}C with distance from shore suggests that the CH_4 pool has been oxidized while traveling away from the littoral. We do not, however, exclude the possibility that the change in isotopic signature of the CH_4 could also be partly due to the addition of CH_4 from other methanogenic pathways. The $\delta^{13}C$ of CH_4 is dependent on the substrate from which it was produced such that CH_4 produced via acetoclasty may have a different $\delta^{13}C$ than that produced via hydrogenotrophy, albeit their signatures overlap on the depleted end (Whiticar, 1999). Oxic CH_4 production in surface waters may also impact the surface CH_4 pool signature, although little is still known about this process (Bižić et al., 2020).

What is obvious though is that there is an overall trend with decreasing concentration and enrichment of $\delta^{13}CH_4$ from the shore toward the center of the lake which implies a high degree of variability in concentration and $\delta^{13}CH_4$ near shore. The variability in concentration is similar to that seen in nearshore sampling in other studies, particularly in vegetated habitats, which may also impact the amount of biological processing occurring in those zones (Desrosiers et al., 2022).

DelSontro, del Giorgio, and Prairie (2018) related $[CH_4]$ and $\delta^{13}CH_4$ from shore to the center of their study lakes using a linear equation that evolved from the development of their lateral CH_4 model (Equation 12 of their work). The high resolution of isotopic and concentration data provided by the MILS instrument, however, suggests that the relationship between isotopic signature and CH_4 concentration from shore to the center of Lake Aiguebelette is not linear (see Figure S7 in Supporting Information S1). The linear relationship holds if only considering littoral measurements (water depth <6 m in this study, Figure S7a in Supporting Information S1) and becomes non-linear when pelagic measurements are included (>6 m, Figure S7a in Supporting Information S1).

The rate coefficient ($k_{O/P}$ $[d^{-1}]$) expressing the net impact of biological processes (oxidation and pelagic production) on surface CH_4 concentrations was calculated using our full data set and only littoral data (water depth < 6m) and a $k_{O/P}$ of 0.640 and 0.273 d^{-1} was obtained, respectively. This is almost a threefold difference that suggests that oxidation is less dominant in just the littoral compared to the littoral plus pelagic surface waters. If instead of using the full high-resolution data set we only use discrete data extracted at the location of Leg A (similar to what DelSontro, del Giorgio, and Prairie (2018) did), then the non-linearity would have not been captured and a $k_{O/P}$ of 0.582 d^{-1} would have been obtained (i.e., similar to using our full littoral plus pelagic data set) but without the non-linearity. The $k_{O/P}$ values we report here are within the range of values obtained for the 12 North American lakes studied in DelSontro, del Giorgio, and Prairie (2018) and confirms that oxidation prevails over pelagic production in Lake Aiguebelette. It seems, however, that the non-linearity presented in our high-resolution data set cannot easily be represented by discrete data. For example, only one of the 12 lakes in DelSontro, del Giorgio, and Prairie (2018) showed the non-linearity (Figure S8 in Supporting Information S1). This non-linearity is an interesting result of using the high-resolution MILS that requires further investigation in order to understand the mechanisms behind it and to improve surface CH_4 modeling.

3.3. A Broader Context for Lake Aiguebelette

A method for retrieving the isotopic signature of the source of the target gas, called the Keeling plot (Keeling, 1958), consists of plotting the $\delta^{13}CH_4$ against the inverse of the dissolved CH_4 concentration and suggests that the isotopic value at the intercept ($1/CH_4 = 0$ mol^{-1} L) corresponds to the situation where the dissolved CH_4 concentrations tend to infinite values (Sasakawa et al., 2008). For our data set, this intercept corresponds to $\delta^{13}CH_4 = -72.85 \pm 1.22‰$ (Figure 6), which lies at the low end of typical values observed in other lakes (e.g., DelSontro, del Giorgio, & Prairie, 2018). The slope of that line ($1{,}887.53 \pm 263.9‰$ nmol L^{-1}) indicates how fast the isotopic signature is changing with respect to the concentration of dissolved CH_4 and provides information about the predominant CH_4 processing occurring (oxidation for positive slope, and production for negative slope), but is also related to other factors such as the possible pathway of CH_4 production, the residence time of the water mass, the presence of different CH_4 inputs, etc.

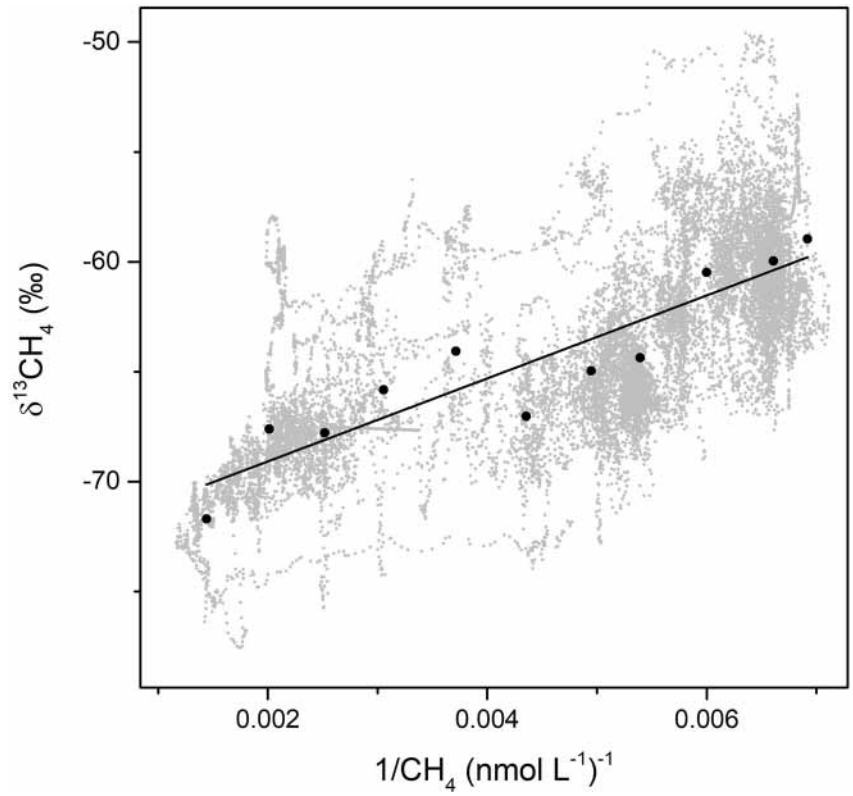

Figure 6. The isotopic composition of dissolved methane ($\delta^{13}CH_4$) plotted against the inverse of the concentration of dissolved CH_4 for continuous (gray dots) and averaged (black dots) surface water data from the campaign. The intercept at $1/CH_4 = 0$ mol^{-1} L is $\delta^{13}CH_4 = -72.85 \pm 1.22$‰ and represents the isotopic signature at the source and the slope ($1{,}887.53 \pm 263.9$‰ nmol L^{-1}) indicating how fast the isotopic signature is changing with respect to the concentration of dissolved CH_4.

In order to investigate the relationship between surface CH_4 and its $\delta^{13}C$ signature, we used the data from 12 Northern American lakes in DelSontro, del Giorgio, and Prairie (2018) and calculated the Keeling slope for each of them. Interestingly, we then found a negative relationship between the absolute value of the Keeling slope and lake area (Figure 7). This relationship is likely explained by the fact that smaller lakes have a larger littoral-to-total area ratio with the littoral zone being the location where a large portion of CH_4 production occurs. Littoral surface waters are not only closest to anoxic sediments where methanogenesis occurs but also to zones of macrophytes that have a significant influence on CH_4 concentrations (Baliña et al., 2022; Bastviken et al., 2023; Desrosiers et al., 2022) and may even contribute to OMP (Hilt et al., 2022). Shallow littoral waters are also more heavily influenced by wind, waves (Bussmann, 2005; Hofmann et al., 2010; Murase et al., 2005), and atmospheric pressure (Joyce & Jewell, 2003; Wik et al., 2013), all of which can enhance CH_4 diffusion and ebullition, and the resulting dissolved CH_4 concentrations in the littoral zone. On the other hand, wind-induced turbulence in littoral zones promotes penetration of oxic water into surficial sediments and subsequently some oxidation in those upper layers, albeit oxygen penetration is usually only a few millimeters and does not often dominate over production and release (Huttunen et al., 2006). The combined impact of these processes suggests that littoral zones are regions of higher CH_4 concentrations due to enhanced release from sediments and higher variability in $\delta^{13}CH_4$ due to the active biogeochemical processing also occurring there. Ultimately, $\delta^{13}CH_4$ variability will be more pronounced in smaller lakes because of that larger littoral fraction (Figure 7), and this is an area of research that would benefit greatly from more high resolution data like that provided by the MILS instrument.

4. Conclusion and Future Works

We used an in situ fast response sensor for continuous, high-resolution measurements of dissolved gases to create a 2D surface map of dissolved CH_4 and $\delta^{13}CH_4$ of the southern portion of Lake Aiguebelette during a

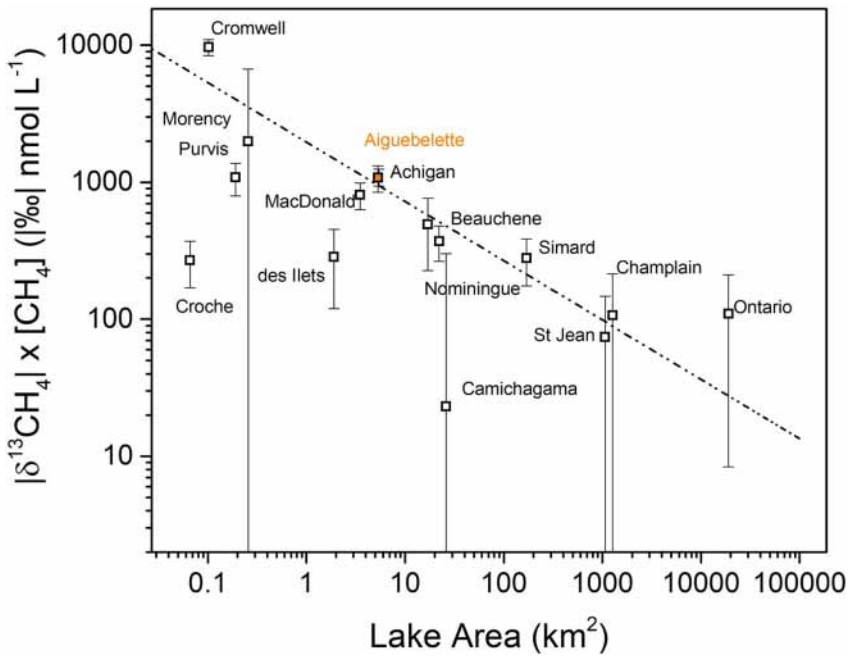

Figure 7. A log-log plot of the absolute value of the slopes calculated while plotting the $\delta^{13}CH_4$ versus the inverse of the CH_4 for the different lakes against the lake area. Data from Lake Aiguebelette (this work) is reported in orange. Data from the other lakes are from DelSontro, del Giorgio, and Prairie (2018). $R^2 = 0.60$.

stratification period. The MILS sensor has an accuracy of ±12% (2σ) for dissolved CH_4 concentration measurements (against ± 5% for discrete measurements) and ±2.6 ‰ and ±6.6 ‰ (2σ) for the $\delta^{13}CH_4$ if referred or not to a standard gas mixture for each deployment, respectively. CH_4 concentration data between discrete samples and the in situ MILS sensor were in good agreement. The isotopic results of the MILS sensor enable the investigation of the biological processing of surface CH_4 at a higher spatial resolution than discrete samples. At Lake Aiguebelette, we can conclude that CH_4 oxidation is the dominant biological process reducing the surface CH_4 pool in spring, and hence reducing some CH_4 emissions. In this work, we were able to compare our surface CH_4 and $\delta^{13}CH_4$ trends with respect to discrete data from 12 other lakes in North America. Lake Aiguebelette data followed the same trend as the majority of these data, with a decreasing CH_4 concentration with distance from shore. The comparison of these data highlights a dependency of the changing rate of isotopic ratio with respect to CH_4 concentration which decreases as a function of lake size. This is related to the fact that smaller lakes tend to have larger biologically active littoral zones relative to total lake area. This multi-lake analysis helps reinforce the reliability of the in situ MILS instrument, which allows for a reduction in measurement time while significantly improving the resolution and spatial coverage of measurements.

This new in situ methodology has several advantages over the traditional water sampling followed by laboratory analysis. First, the MILS sensor allows higher spatial resolution because it is not limited by the number of samples and time for the analysis. This spatial resolution is especially important for the littoral zone, which shows a high degree of variability both in terms of CH_4 concentration and isotopic signatures. The in situ instrument provides therefore a more representative estimate of a water body than discrete sampling. Secondly, the MILS sensor avoids possible artifacts due to outgassing during water sampling as well as degradation of the sample during storage (e.g., bacterial degradation or outgassing due to possible leaks). Finally, the fast deployment of the MILS system means that it is easier to conduct regular surveys and better resolve seasonal trends in aquatic CH_4. Although not illustrated in this study, the MILS sensor also allows in situ measurement with depth. Thus, vertical profiles at multiple locations could be conducted to better constrain CH_4 dynamics and the migration of water masses, as well as provide a more comprehensive view of how CH_4 contributes to the carbon cycle in aquatic systems.

Data Availability Statement

Data can be found in the following repository: https://doi.org/10.17632/djjd6pdhm9.2 (Grilli, 2023).

Acknowledgments
This study was funded by agreement N° FUGA-UGA-2019-001 between University Grenoble Alpes Fundation and EDF and by the French National Program (ANR) "Investment for Future - Excellency Equipment" project TERRA FORMA with the reference ANR-21-ESRE-0014 ". The optical spectrometer of the MILS and the work carried out at IGE was financed thought the European Community's Seventh Framework Programme ERC-2015-PoC under grant agreement no. 713619 (ERC OCEAN-IDs), the Agence Nationale de la Recherche (ANR) under grant agreement ANR-18-CE04-0003-01 (SWIS), with support from the SATT Linksium of Grenoble, France, of the Service Partenariat & Valorisation (SPV) of the CNRS. We thank the Communité de Commune du Lac d'Aiguebellete (CCLA) for the loan of the electric boat to carry out the sampling campaign, and Arthaud's family for their nice house nearby the lake. The authors would like to thank students and staff at IGE laboratory, Constantin Schwarze, Romain Biron and Guilhem Freche, for their contribution during field trip. We thank Anunciacion Martinez and Benjamin Mercier for the analysis of GHGs in METIS Laboratory. We thank Frederic Guerin from GET Lab, Véronique Vaury and Sylvain Huon from iEES lab and Didier Jezequel from IPGP currently at INRAE for the fruitful discussions.

References

Abril, G., & Iversen, N. (2002). Methane dynamics in a shallow non-tidal estuary (Randers Fjord, Denmark). *Marine Ecology Progress Series*, *230*, 171–181. https://doi.org/10.3354/meps230171

Baliña, S., Sánchez, M. L., & del Giorgio, P. A. (2022). Physical factors and microbubble formation explain differences in CH4 dynamics between shallow lakes under alternative states. *Frontiers of Environmental Science*, *10*(June), 1–11. https://doi.org/10.3389/fenvs.2022.892339

Bärenbold, F., Boehrer, B., Grilli, R., Mugisha, A., von Tümpling, W., Umutoni, A., & Schmid, M. (2020). In S. A. Loiselle (Eds.), *No increasing risk of a limnic eruption at Lake Kivu: Intercomparison study reveals gas concentrations close to steady state* (Vol. 15, p. e0237836). https://doi.org/10.1371/journal.pone.0237836

Bastviken, D., Cole, J., Pace, M., & Tranvik, L. (2004). Methane emissions from lakes: Dependence of lake characteristics, two regional assessments, and a global estimate. *Global Biogeochemical Cycles*, *18*(4), 1–12. https://doi.org/10.1029/2004GB002238

Bastviken, D., Cole, J. J., Pace, M. L., & Van de Bogert, M. C. (2008). Fates of methane from different lake habitats: Connecting whole-lake budgets and CH4 emissions. *Journal of Geophysical Research*, *113*(G2), G02024. https://doi.org/10.1029/2007JG000608

Bastviken, D., Ejlertsson, J., & Tranvik, L. (2002). Measurement of methane oxidation in lakes: A comparison of methods. *Environmental Science & Technology*, *36*(15), 3354–3361. https://doi.org/10.1021/es010311p

Bastviken, D., Treat, C. C., Pangala, S. R., Gauci, V., Enrich-Prast, A., Karlson, M., et al. (2023). The importance of plants for methane emission at the ecosystem scale. *Aquatic Botany*, *184*, 103596. https://doi.org/10.1016/j.aquabot.2022.103596

Bižić, M., Klintzsch, T., Ionescu, D., Hindiyeh, M. Y., Günthel, M., Muro-Pastor, A. M., et al. (2020). Aquatic and terrestrial cyanobacteria produce methane. *Science Advances*, *6*(3), eaax5343. https://doi.org/10.1126/sciadv.aax5343

Brennwald, M. S., Schmidt, M., Oser, J., & Kipfer, R. (2016). A portable and autonomous mass spectrometric system for on-site environmental gas analysis. *Environmental Science & Technology*, *50*(24), 13455–13463. https://doi.org/10.1021/acs.est.6b03669

Bussmann, I. (2005). Methane release through resuspension of littoral sediment. *Biogeochemistry*, *74*(3), 283–302. https://doi.org/10.1007/s10533-004-2223-2

CCLA. (2017). *Community of Communes of Lac d'Aiguebelette, Etude des impacts des Act*. Anthr. sur les enjeux Conserv. Retrieved from https://ccla.fr/

Claypool, G. E., & Kvenvolden, K. A. (1983). Methane and other hydrocarbon gases in marine sediment. *Annual Review of Earth and Planetary Sciences*, *11*(1), 299–327. https://doi.org/10.1146/annurev.ea.11.050183.001503

DelSontro, T., Beaulieu, J. J., & Downing, J. A. (2018). Greenhouse gas emissions from lakes and impoundments: Upscaling in the face of global change. *Limnology and Oceanography Letters*, *3*(3), 64–75. https://doi.org/10.1002/lol2.10073

DelSontro, T., del Giorgio, P. A., & Prairie, Y. T. (2018). No longer a paradox: The interaction between physical transport and biological processes explains the spatial distribution of surface water methane within and across lakes. *Ecosystems*, *21*(6), 1073–1087. https://doi.org/10.1007/s10021-017-0205-1

Desrosiers, K., DelSontro, T., & del Giorgio, P. A. (2022). Disproportionate contribution of vegetated habitats to the CH4 and CO2 budgets of a boreal lake. *Ecosystems*, *25*(7), 1522–1541. https://doi.org/10.1007/s10021-021-00730-9

Donis, D., Flury, S., Stöckli, A., Spangenberg, J. E., Vachon, D., & McGinnis, D. F. (2017). Full-scale evaluation of methane production under oxic conditions in a mesotrophic lake. *Nature Communications*, *8*(1), 1661. https://doi.org/10.1038/s41467-017-01648-4

Etminan, M., Myhre, G., Highwood, E. J., & Shine, K. P. (2016). Radiative forcing of carbon dioxide, methane, and nitrous oxide: A significant revision of the methane radiative forcing. *Geophysical Research Letters*, *43*(24), 12614–12623. https://doi.org/10.1002/2016GL071930

Gaillard, J. F., Sarazin, G., Pauwels, H., Philippe, L., Lavergne, D., & Blake, G. (1987). Interstitial water and sediment chemistries of Lake Aiguebelette (savoy, France). *Chemical Geology*, *63*(1–2), 73–84. https://doi.org/10.1016/0009-2541(87)90075-1

Garnier, J., Vilain, G., Silvestre, M., Billen, G., Jehanno, S., Poirier, D., et al. (2013). Budget of methane emissions from soils, livestock and the river network at the regional scale of the Seine basin (France). *Biogeochemistry*, *116*(1–3), 199–214. https://doi.org/10.1007/s10533-013-9845-1

Gerardo-Nieto, O., Vega-Peñaranda, A., Gonzalez-Valencia, R., Alfano-Ojeda, Y., & Thalasso, F. (2019). Continuous measurement of diffusive and ebullitive fluxes of methane in aquatic ecosystems by an open dynamic chamber method. *Environmental Science & Technology*, *53*(9), 5159–5167. https://doi.org/10.1021/acs.est.9b00425

Gonzalez-valencia, R., Magana-rodriguez, F., Gerardo-nieto, O., Sepulveda-jauregui, A., Martinez-cruz, K., Anthony, K. W., et al. (2014). In situ measurement of dissolved methane and carbon dioxide in freshwater ecosystems by O ff -Axis integrated cavity output spectroscopy.

Grilli, R. (2023). High-resolution, in situ measurement of dissolved CH4, d13CH4 and C2H6 at Lake Aiguebelette using a membrane inlet laser spectrometer. Mendeley Data. V2 [Dataset]. https://doi.org/10.17632/djjd6pdhm9.2

Grilli, R., Darchambeau, F., Chappellaz, J., Mugisha, A., Triest, J., & Umutoni, A. (2020). Continuous in situ measurement of dissolved methane in Lake Kivu using a membrane inlet laser spectrometer. *Geoscientific Instrumentation, Methods and Data Systems*, *9*(1), 141–151. https://doi.org/10.5194/gi-9-141-2020

Grilli, R., Triest, J., Chappellaz, J., Calzas, M., Desbois, T., Jansson, P., et al. (2018). Sub-Ocean: Subsea dissolved methane measurements using an embedded laser spectrometer technology. *Environmental Science & Technology*, *52*(18), 10543–10551. https://doi.org/10.1021/acs.est.7b06171

Grossart, H.-P., Frindte, K., Dziallas, C., Eckert, W., & Tang, K. W. (2011). Microbial methane production in oxygenated water column of an oligotrophic lake. *Proceedings of the National Academy of Sciences*, *108*(49), 19657–19661. https://doi.org/10.1073/pnas.1110716108

Gudasz, C., Bastviken, D., Steger, K., Premke, K., Sobek, S., & Tranvik, L. J. (2010). Temperature-controlled organic carbon mineralization in lake sediments. *Nature*, *466*(7305), 478–481. https://doi.org/10.1038/nature09186

Günthel, M., Donis, D., Kirillin, G., Ionescu, D., Bizic, M., McGinnis, D. F., et al. (2019). Contribution of oxic methane production to surface methane emission in lakes and its global importance. *Nature Communications*, *10*(1), 5497. https://doi.org/10.1038/s41467-019-13320-0

Hilt, S., Grossart, H., McGinnis, D. F., & Keppler, F. (2022). Potential role of submerged macrophytes for oxic methane production in aquatic ecosystems. *Limnology & Oceanography*, *67*(S2), 1–13. https://doi.org/10.1002/lno.12095

Hofmann, H., Federwisch, L., & Peeters, F. (2010). Wave-induced release of methane: Littoral zones as source of methane in lakes. *Limnology & Oceanography*, *55*(5), 1990–2000. https://doi.org/10.4319/lo.2010.55.5.1990

Huttunen, J. T., Väisänen, T. S., Hellsten, S. K., & Martikainen, P. J. (2006). Methane fluxes at the sediment–water interface in some boreal lakes and reservoirs. *Boreal Environment Research*, *11*(1), 27.

Joyce, J., & Jewell, P. W. (2003). Physical controls on methane ebullition from reservoirs and lakes. *Environmental and Engineering Geoscience*, *9*(2), 167–178. https://doi.org/10.2113/9.2.167

Juutinen, S., Alm, J., Larmola, T., Huttunen, J. T., Morero, M., Martikainen, P. J., & Silvola, J. (2003). Major implication of the littoral zone for methane release from boreal lakes. *Global Biogeochemical Cycles*, *17*(4). https://doi.org/10.1029/2003GB002105

Juutinen, S., Rantakari, M., Kortelainen, P., Huttunen, J. T., Larmola, T., Alm, J., et al. (2009). Methane dynamics in different boreal lake types. *Biogeosciences*, *6*(2), 209–223. https://doi.org/10.5194/bg-6-209-2009

Keeling, C. D. (1958). The concentration and isotopic abundances of atmospheric carbon dioxide in rural areas. *Geochimica et Cosmochimica Acta*, *13*(4), 322–334. https://doi.org/10.1016/0016-7037(58)90033-4

Koné, Y. J. M., Abril, G., Delille, B., & Borges, A. V. (2010). Seasonal variability of methane in the rivers and lagoons of ivory coast (west africa). *Biogeochemistry*, *100*(1–3), 21–37. https://doi.org/10.1007/s10533-009-9402-0

Lechevallier, L., Grilli, R., Kerstel, E., Romanini, D., & Chappellaz, J. (2019). Simultaneous detection of C2H6, CH4, and δ13C-CH4 using optical feedback cavity-enhanced absorption spectroscopy in the mid-infrared region: Towards application for dissolved gas measurements. *Atmospheric Measurement Techniques*, *12*(6), 3101–3109. https://doi.org/10.5194/amt-12-3101-2019

Loken, L. C., Crawford, J. T., Schramm, P. J., Stadler, P., Desai, A. R., & Stanley, E. H. (2019). Large spatial and temporal variability of carbon dioxide and methane in a eutrophic lake. *Journal of Geophysical Research: Biogeosciences*, *124*(7), 2248–2266. https://doi.org/10.1029/2019JG005186

MacIntyre, S., & Melack, J. M. (1995). Vertical and horizontal transport in lakes: Linking littoral, benthic, and pelagic habitats. *Journal of the North American Benthological Society*, *14*(4), 599–615. https://doi.org/10.2307/1467544

Maher, D. T., Cowley, K., Santos, I. R., Macklin, P., & Eyre, B. D. (2015). Methane and carbon dioxide dynamics in a subtropical estuary over a diel cycle: Insights from automated in situ radioactive and stable isotope measurements. *Marine Chemistry*, *168*, 69–79. https://doi.org/10.1016/j.marchem.2014.10.017

Maier, M. S., Canning, A. R., Brennwald, M. S., Teodoru, C. R., & Wehrli, B. (2022). Spatial mapping of dissolved gases in the danube delta reveals intense plant-mediated gas transfer. *Frontiers of Environmental Science*, *10*(March), 1–16. https://doi.org/10.3389/fenvs.2022.838126

McAullife, C. (1971). *GC determination of solutes by multiple phase equilibration* (pp. 46–51). Chem Tech.

McMutrtry, G. M., Wiltshire, J. C., & Bossuyt, A. (2005). Hydrocarbon seep monitoring using in situ deep sea mass spectrometry. *Ocean*, *1*, 395–400. https://doi.org/10.1109/OCEANSE.2005.1511747

Milberg, P., Törnqvist, L., Westerberg, L. M., & Bastviken, D. (2017). Temporal variations in methane emissions from emergent aquatic macrophytes in two boreonemoral lakes. *AoB Plants*, *9*(4). https://doi.org/10.1093/aobpla/plx029

Morville, J., Romanini, D., & Kerstel, E. (2014). In G. Gagliardi & H.-P. Loock (Eds.), *Cavity-enhanced spectroscopy and sensing*. Springer Berlin Heidelberg.

Murase, J., Sakai, Y., Kametani, A., & Sugimoto, A. (2005). Dynamics of methane in mesotrophic lake biwa, Japan. *Ecological Research*, *20*(3), 377–385. https://doi.org/10.1007/s11284-005-0053-x

Murase, J., Sakai, Y., Sugimoto, A., Okubo, K., & Sakamoto, M. (2003). Sources of dissolved methane in lake biwa. *Limnology*, *4*(2), 91–99. https://doi.org/10.1007/s10201-003-0095-0

Myhre, G., Shindell, D., Bréon, F.-M., Collins, W., Fuglestvedt, J., Huang, J., et al. (2013). Anthropogenic and natural radiative forcing. In T. Stocker, D. Qin, G.-K. Plattner, M. Tignor, S. K. Allen, J. Boschung et al. (Eds.), *Climate change 2013: The Physical Science Basis. Contribution of Working Group I to the Fifth Assessment Report of the Intergovernmental Panel on climate change* (pp. 659–740). Cambridge University Press.

NINH. (2016). National inventory of natural heritage. [online] Retrieved from Retrieved from https://inpn.mnhn.fr/site/natura2000/FR8201770

OLA. (2022). Observatory on lake. Retrieved from https://www6.inrae.fr/soere-ola_eng

Ordóñez, C., DelSontro, T., Langenegger, T., Donis, D., Suarez, E. L., & McGinnis, D. F. (2023). Evaluation of the methane paradox in four adjacent pre-alpine lakes across a trophic gradient. *Nature Communications*, *14*(1), 2165. https://doi.org/10.1038/s41467-023-37861-7

Phillips, N. G., Ackley, R., Crosson, E. R., Down, A., Hutyra, L. R., Brondfield, M., et al. (2013). Mapping urban pipeline leaks: Methane leaks across Boston. *Environmental Pollution*, *173*, 1–4. https://doi.org/10.1016/j.envpol.2012.11.003

Rasilo, T., Prairie, Y. T., & del Giorgio, P. A. (2015). Large-scale patterns in summer diffusive CH4 fluxes across boreal lakes, and contribution to diffusive C emissions. *Global Change Biology*, *21*(3), 1124–1139. https://doi.org/10.1111/gcb.12741

Rimet, F., Anneville, O., Barbet, D., Chardon, C., Crépin, L., Domaizon, I., et al. (2020). The Observatory on LAkes (OLA) database: Sixty years of environmental data accessible to the public. *Journal of Limnology*, *79*(2), 164–178. https://doi.org/10.4081/jlimnol.2020.1944

Robb, W. L. (1968). Thin silicon membranes. Their permeation properties and some applications. *Annals of the New York Academy of Sciences*, *146*(1), 119–137. https://doi.org/10.1111/j.1749-6632.1968.tb20277.x

Rosentreter, J. A., Borges, A. V., Deemer, B. R., Holgerson, M. A., Liu, S., Song, C., et al. (2021). Half of global methane emissions come from highly variable aquatic ecosystem sources. *Nature Geoscience*, *14*(4), 225–230. https://doi.org/10.1038/s41561-021-00715-2

Sander, R. (2015). Compilation of Henry 's law constants (version 4.0) for water as solvent. *Atmospheric Chemistry and Physics*, *15*(8), 4399–4981. https://doi.org/10.5194/acp-15-4399-2015

Sasakawa, M., Tsunogai, U., Kameyama, S., Nakagawa, F., Nojiri, Y., & Tsuda, A. (2008). Carbon isotopic characterization for the origin of excess methane in subsurface seawater. *Journal of Geophysical Research*, *113*(C3), C03012. https://doi.org/10.1029/2007JC004217

Saunois, M., Stavert, A. R., Poulter, B., Bousquet, P., Canadell, J. G., Jackson, R. B., et al. (2019). The global methane budget 2000-2017. *Earth System Science Data*, *12*(3), 1561–1623. https://doi.org/10.5194/essd-2019-128

Short, R. T., Toler, S. K., Kibelka, G. P. G., Rueda Roa, D. T., Bell, R. J., & Byrne, R. H. (2006). Detection and quantification of chemical plumes using a portable underwater membrane introduction mass spectrometer. *Trends in Analytical Chemistry (Reference Ed.)*, *25*(7), 637–646. https://doi.org/10.1016/j.trac.2006.05.002

Steinsberger, T., Schwefel, R., Wüest, A., & Müller, B. (2020). Hypolimnetic oxygen depletion rates in deep lakes: Effects of trophic state and organic matter accumulation. *Limnology & Oceanography*, *65*(12), 3128–3138. https://doi.org/10.1002/lno.11578

Tortell, P. D. (2005). Dissolved gas measurements in oceanic waters made by membrane inlet mass spectrometry. *Limnology and Oceanography: Methods*, *3*(1), 24–37. https://doi.org/10.4319/lom.2005.3.24

Tranvik, L. J., Downing, J. A., Cotner, J. B., Loiselle, S. A., Striegl, R. G., Ballatore, T. J., et al. (2009). Lakes and reservoirs as regulators of carbon cycling and climate. *Limnology & Oceanography*, *54*(6), 2298–2314. https://doi.org/10.4319/lo.2009.54.6_part_2.2298

Triest, J., Chappellaz, J., & Grilli, R. (2017). *Patent WO2018127516A1: System for fast and in-situ sampling of dissolved gases in the ocean*. CNRS, Grenoble FRANCE).

Vachon, D., Langenegger, T., Donis, D., & McGinnis, D. F. (2019). Influence of water column stratification and mixing patterns on the fate of methane produced in deep sediments of a small eutrophic lake. *Limnology & Oceanography*, *64*(5), 2114–2128. https://doi.org/10.1002/lno.11172

Wankel, S. D., Huang, Y., Gupta, M., Provencal, R., Leen, J. B., Fahrland, A., et al. (2013). Characterizing the distribution of methane sources and cycling in the deep sea via in situ stable isotope analysis. *Environmental Science & Technology*, *47*(3), 1478–1486. https://doi.org/10.1021/es303661w

Webb, J. R., Maher, D. T., & Santos, I. R. (2016). Automated, in situ measurements of dissolved CO2, CH4, and δ13C values using cavity enhanced laser absorption spectrometry: Comparing response times of air-water equilibrators. *Limnology and Oceanography: Methods*, *14*(5), 323–337. https://doi.org/10.1002/lom3.10092

Whiticar, M. J. (1999). Carbon and hydrogen isotope systematics of bacterial formation and oxidation of methane. *Chemical Geology*, *161*(1), 291–314. https://doi.org/10.1016/S0009-2541(99)00092-3

Wik, M., Crill, P. M., Varner, R. K., & Bastviken, D. (2013). Multiyear measurements of ebullitive methane flux from three subarctic lakes. *Journal of Geophysical Research: Biogeosciences*, *118*(3), 1307–1321. https://doi.org/10.1002/jgrg.20103

Yuan, F., Hu, M., He, Y., Chen, B., Yao, L., Xu, Z., & Kan, R. (2020). Development of an in situ analysis system for methane dissolved in seawater based on cavity ringdown spectroscopy Development of an in situ analysis system for methane dissolved in seawater based on cavity ringdown spectroscopy. *Review of Scientific Instruments*, *91*(083106). https://doi.org/10.1063/5.0004742

Yvon-Durocher, G., Allen, A. P., Bastviken, D., Conrad, R., Gudasz, C., St-Pierre, A., et al. (2014). Methane fluxes show consistent temperature dependence across microbial to ecosystem scales. *Nature*, *507*(7493), 488–491. https://doi.org/10.1038/nature13164

Zhang, W., Li, H., Pueppke, S. G., & Pang, J. (2021). Restored riverine wetlands in a headwater stream can simultaneously behave as sinks of N2O and hotspots of CH4 production. *Environmental Pollution*, *284*, 117114. https://doi.org/10.1016/j.envpol.2021.117114

References From the Supporting Information

Encinas Fernández, J., Peeters, F., & Hofmann, H. (2016). On the methane paradox: Transport from shallow water zones rather than in situ methanogenesis is the major source of CH4 in the open surface water of lakes. *Journal of Geophysical Research: Biogeosciences*, *121*(10), 2717–2726. https://doi.org/10.1002/2016JG003586

Rimet, F., Khac, V. T., Quétin, P., & De, S. (2019). Suivi de la qualité des eaux du lac d'Aiguebelette.